PARTICLE IMAGE VELOCIMETRY IN THE EXHAUST OF SMALL SOLID ROCKET MOTORS

B.J. BALAKUMAR[(1)] and R.J. ADRIAN[(2)]
Laboratory for Turbulence and Complex Flows
Department of Theoretical and Applied Mechanics
University of Illinois, Urbana, IL 61801
[(1)]Email: bbalasub@uiuc.edu
[(2)]Email: r-adrian@uiuc.edu

ABSTRACT

Combusting environments where high velocities are encountered present a very challenging environment for the application of the Particle image Velocimetry (PIV) method. The physical features of the flow - background irradiance from burning gases, dense smoke, compressibility effects, inability to control seeding densities and inherent CCD limitations - make the measurement process difficult in the exhaust plume of solid rocket motors. A precisely controlled optical shutter-the Liquid Crystal Variable Attenuator (LCVA)- was used to control the light intensity reaching the CCD. The use of the LCVA alleviates the CCD limitations and permits a cross-correlation of images even in the presence of strong background irradiation. Phase averaged velocity fields were obtained in the unsteady rocket flow, by controlling the start of the triggering sequence using a photo-detector placed at the nozzle exit and interfacing it to the synchronizer (Fig. 1). Peak centerline velocities of more than 600 m/s were measured in burning particle laden gas flows at temperatures exceeding 2500K. Self-similarity of the mean turbulent velocity has been observed despite the complicated character of the flow.

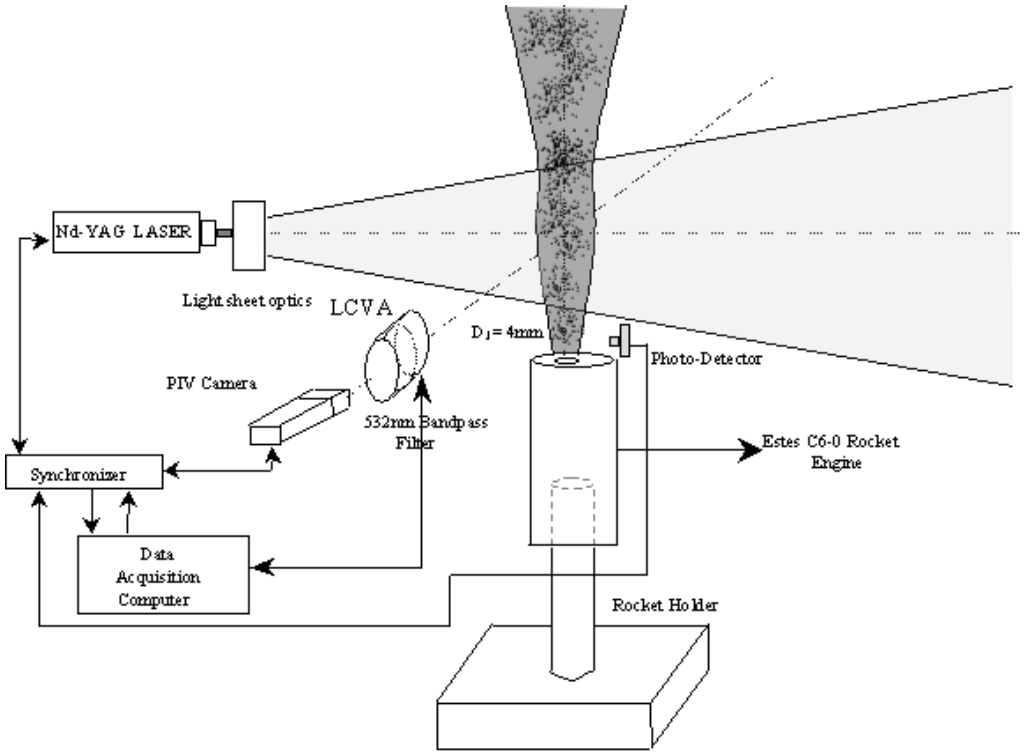

Figure 1. A schematic of the experimental setup (not to scale)

1. INTRODUCTION

The physics of operation of an SRM are immensely complicated. The limited number of observable variables makes its understanding difficult. Time histories of the head end pressure measurements are the typical and most often, the only data available for these rocket engines. Occasionally, the particulate concentrations at the exhaust and single point velocity measurements are also available (Christodoulou et all, 2002). However, the prohibitive costs of repeatedly firing a motor to obtain velocities at several points can be reduced by the use of planar velocity measurement techniques. Measurements of the mean and turbulence velocity statistics inside the plume would provide invaluable insights into the events that happen within a Solid Rocket Motor. An analysis of the evolution of these velocity fields would also serve to diagnose faulty or off-design operations in SRMs. The PIV method is an effective and efficient tool to accomplish this since it serves the dual purposes of measuring the velocities as well as the particulate concentrations inside the plume. The information gathered would serve as a valuable reference for validating the whole-system simulation efforts of solid rocket motors under both normal and abnormal operating conditions.

Previous studies have largely been limited to the analysis of the scattering characteristics (Yan et all, 1993) and measurements of particulates in the exhaust plume (Edwards et al, 1986). More recently, single-point velocity measurements were made using a Phase-doppler particle sizing technique (Christodoulou et all, 2002). By controlling the seeding inside an experimental combustion chamber, velocity measurements of around 60 m/s were made in the exhaust as detailed in Deimling L., 1999. The present experiment seeks to establish the possibilities of making PIV measurements, in these harsh environments and to optimize the yield of planar vector fields, even in the complete absence of control over the seeding density, while also extending the previously obtainable PIV velocity range in combustion plumes by an order of magnitude. The accuracy of the measurements are affected by the ability of the particles to follow the compressible flow (Urban and Mungal, 1997), non-homogeneity and time dependence of the refractive index of the burning gases and thermophoretic forces (Stella et all, 2001). The presence of expansion and compression waves also leads to a reduction in the number of good vectors, due to their effect on the seeding particulate concentration.

2. EXPERIMENTAL SETUP and TECHNIQUES

2.1 Model Rockets

Estes C6-0 rockets with a rated mean thrust of 5.8N, a total impulse of 10Ns and a nominal 1.7s duration of burn were used in these experiments. A burn length of 2.2 seconds was observed during actual measurements in the laboratory. Thus each firing of the rocket motor provided 33 image pairs at an image capture rate of 15Hz.

Black powder (70-75% Potassium Nitrate, 10-15% Sulphur, 10-15% Charcoal) is used as the propellant. Sulphur fuel is mixed with Potassium Nitrate, which acts as the oxidizer. The charcoal is used to moderate the reactivity of the mixture.

A ceramic nozzle, roughly contoured as a converging-diverging section accelerates the hot gases liberated by the burning of the propellant inside the core of the rocket. The length of the nozzle is not long enough, so the gases coming out of the nozzle are under-expanded. The nozzle diameter at the exit was 4mm. The grain of the propellant becomes that of an end-burner configuration during the neutral burn phase (the phase of the firing during which the engine generates a constant thrust). Thus, temporal averages can be computed between t= 0.7s and t=2.1s. An igniter placed into the nozzle and connected to the ignition system through a cable starts the motor. As the motor starts burning, the igniter and the cable are thrown aside and do not interfere with the flow anymore. The schematic of the rocket is shown in the inset of Fig. 2. and a sequence of photo captures from a typical rocket firing is shown in Fig. 3.

2.2 PIV System and Rocket Setup

A Gemini-PIV Nd-YAG laser rated to generate 5ns pulses with 500mJ of energy at 15Hz was used to provide the illumination. Optics in front of the laser head converted the laser beam into a light sheet of 1mm thickness. A TSI 10-30 PIV camera with 1012 X 1000 pixel CCD chip, placed at 90^0 to the light sheet was used to image an area of 36.2mm X 35.6mm. The camera was operated in the frame-straddle mode with a $\Delta t = 0.8\mu s$. A TSI LaserPulse synchronizer triggered the camera and the laser systems. A photo-detector circuit placed near the nozzle exit is interfaced to the synchronizer to start the imaging sequence at the same

instant of time during each firing, when the rocket starts to spout out the combustion products (Fig. 1). A Liquid Crystal Variable Attenuator was placed in front of the camera to control the amount of light entering the camera during the each frame of the image recording.

The rocket motor was held stationary by a center-chuck mounted on a linear translation stage, which in turn was mounted on a 3 degree-of-freedom pan head. Such a setup simplified the laborious process of aligning the nozzle axis along the laser sheet. The PIV measurements were taken in a plane passing through the axis of the nozzle.

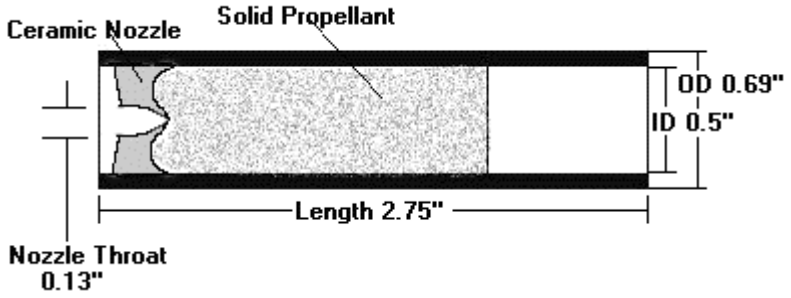

Figure 2. Estes C6-0 Solid Rocket Motor. After ignition, the flame front propagates from left to right in the propellant

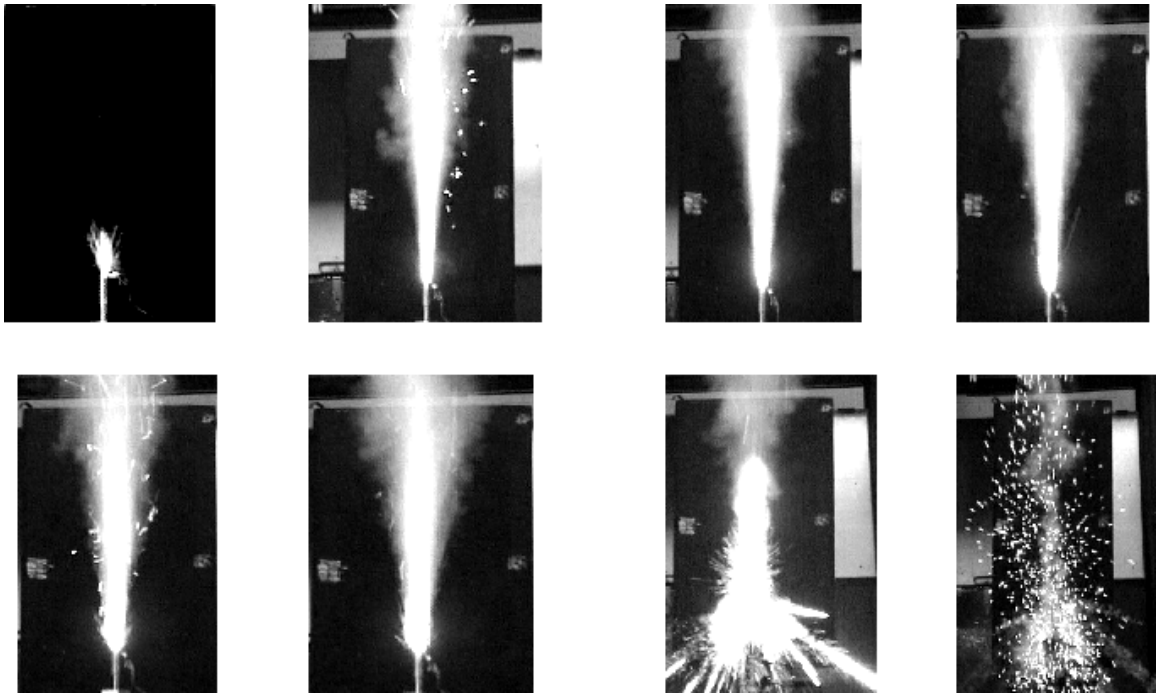

Figure 3. A typical firing sequence from the rocket. The sequence starts at the top left, traversing row 1 and ending at the bottom right picture.

2.3 Liquid Crystal Variable Attenuator

The signals in the frame of a conventional PIV system consist of light scattered off the seeding particles, with the fluid flow medium scattering little or no light at all. However, in the exhaust of an SRM,

the non-uniform time-dependent radiation from the burning gases and incandescence from the fine-smoke particles combine to add noise to the signal scattered by the particles. This decreases the signal-to-noise ratio (SNR) to the extent where it becomes difficult to distinguish the particles from the burning flow. However, by selecting a suitable f#, after providing for depth of field considerations, one can find the optimal laser intensity for the best possible imaging. A 532nm band-pass filter with a bandwidth of 10nm was used to filter out the spectrum of the background light that is different from the laser-light frequency, thereby increasing the SNR. This arrangement is good enough for obtaining vector fields using auto-correlation.

Due to the presence of a large concentration of particles in the exhaust jet of the rockets under consideration, cross-correlation turned out to be more efficient. But the second frame was observed to always saturate providing no vectors in the core region of the jet. The acquisition cameras used in the experiment keep the shutter open for 33.33 ms during the second frame. This is the time needed to transfer all the charge in the on-chip storage, gained by transfer after the 1st frame, to the computer. The corresponding delay for the first frame is 255μs, which is the time needed to transfer all the charge from the electron well in the chip to the storage location. Thus, about 150 times more light is admitted in the second frame thereby saturating the CCD near the core jet region. This eliminates the possibility of obtaining velocity vectors inside the burning jet. This limitation was overcome by the use of a Liquid Crystal Variable Attenuator (LCVA), which acted as a shutter to shorten the exposure during the second frame. The timing diagram of the LCVA is provided below in relation to the PIV camera and lasers. An explanation of the operation of the LCVA follows.

Figure 4. Timing diagram for the PIV setup also showing the operation cycle of the LCVA

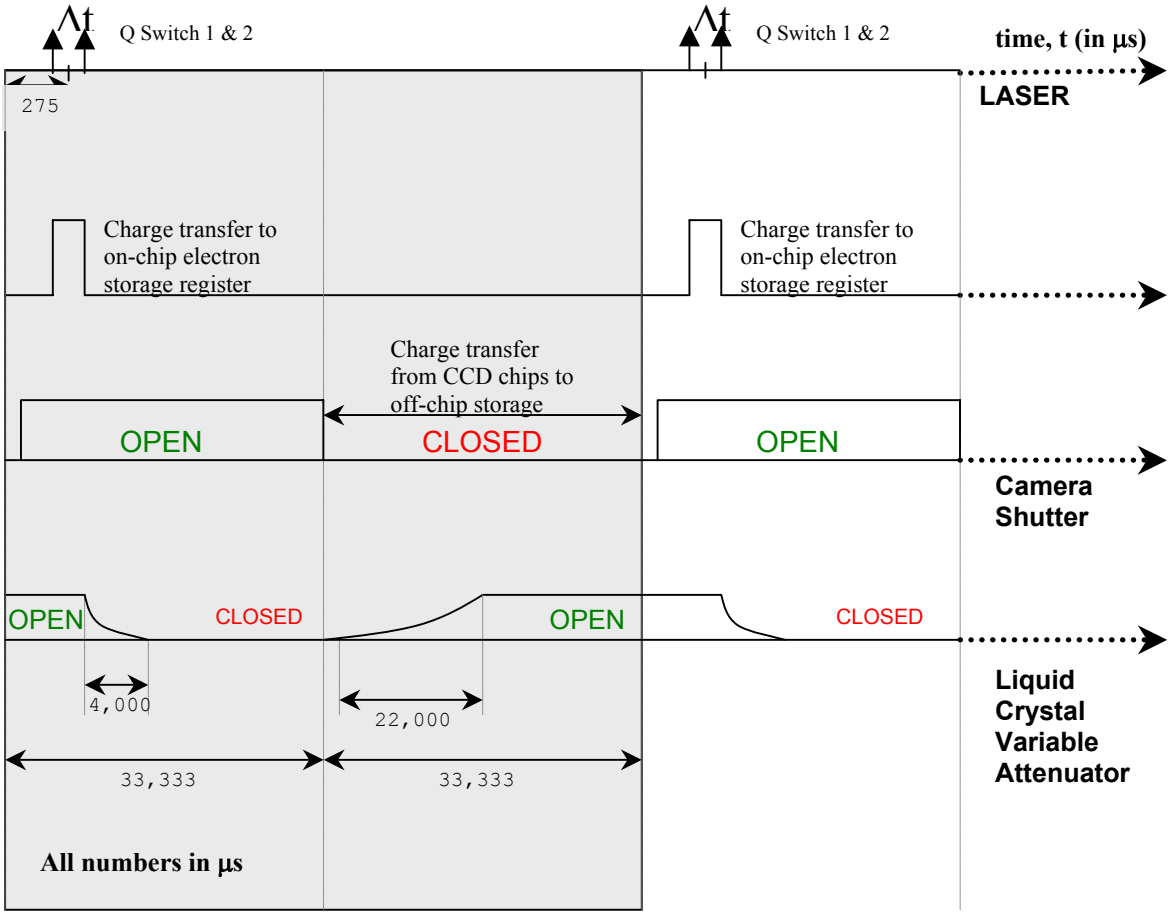

The LCVA consists of a Liquid Crystal Variable Retarder operating between two crossed linear polarizers. The retardance of the retarder is a function of the amplitude of a 2KHz square wave applied to the device. Thus, modulating the amplitude of the AC voltage applied to the retarder varies the retardance, changing the transmission of the LCVA from minimum to a maximum and vice versa. Suitably triggering these transitions, using an in-house developed circuit and a DG535 Four Channel Digital Delay/Pulse Generator, shuts off the light input into the CCD reducing the light allowed into the second frame. It should

be noted that the output stage of the electronics has a low pass filter to remove any DC voltage fed into the LCVA. These operations are shown in Fig. 4.

2.4 Seeding Considerations

The seeding inside the plume was provided by the particles created during the combustion process and ejected out of the nozzle. These particles consist of burning/burnt byproducts of the combustion process in the core of the engine. A Laskin nozzle-based oil atomizer (Meinhart 1994) generating olive oil droplets of 1-2μm diameter was used to provide seeding outside the plume in order to capture the entrainment velocity field.

3. RESULTS

Measurements were taken in a 36.2mm X 35.6mm region, 15.5 nozzle diameters downstream from the nozzle exit. Interrogations were performed with a first window size of 32 X 32 and a second window size of 64 X 64. The region of interest is located below the mach disc, which occurs at the end of the contraction in the jet diameter (Fig. 5).

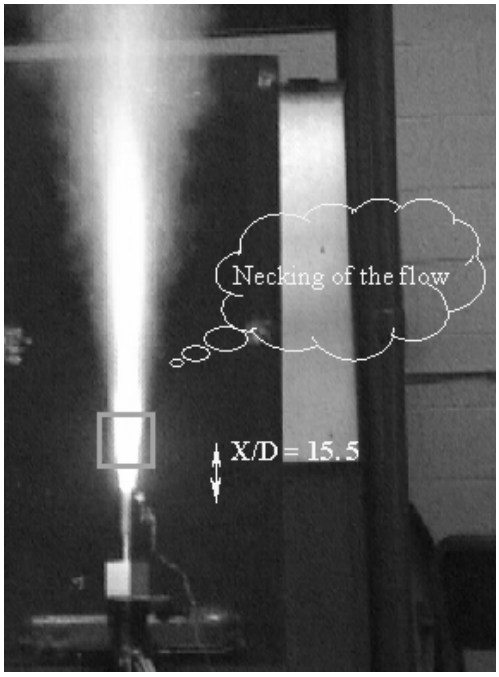

Figure 5. Region of Interest and necking

A typical PIV realization shortly after the start of the firing is shown in Fig. 6. The entrainment caused by the jet can be clearly seen by the whorl near the lower portion of the jet. Ensemble averaged whole-field velocity vectors at t=1.2s along with the thrust-time curve (inset) are shown in Fig. 7. The peak centerline velocities measured were 636 m/s and the centerline velocity is observed to reduce along the axis, away from the nozzle as expected from the decaying jet. In the individual vector fields in each firing, about 15% of the velocity vectors were lost in the core region. This loss was found to be associated with the extreme regions of very high particulate concentrations as well as regions of very low concentrations. This particulate bunching effect is shown in the contrast-enhanced image of Fig. 8.

Mean velocity profiles, normalized with respect to the centerline velocities, were calculated from 15 firings. In order to alleviate the effect of the loss of vectors due to the bunching of particles, velocity averaging was done over 1.5D along the axis of the jet. Through this distance the divergence of the jet was found to be within the spatial resolution of the PIV system. A plot of the normalized ensemble averaged axial velocity as a function of the radial distance, r, normalized with respect to the distance from the nozzle, x, is shown in Fig. 9. The shape of the curves and their similarity when scaled by the length scale ‘x’ is surprisingly like that of an isothermal, incompressible, single phase round jet.

CONCLUSIONS

Very high temperatures, speeds in excess of 600m/s, irradiance from burning particles, dense smoke, inability to control the seeding density and inherent camera limitations render studies of the exhaust jet of solid rocket motors a challenging proposition. A liquid crystal variable attenuator is used to diminish the effect of background illumination. A Laskin nozzle atomizer was used to seed the surrounding fluid in order to observe the entrainment and a very small Δt allowed the capture of high velocities.

The first results arising from this study show that the particles coming out of the rocket nozzle are optically suitable for obtaining PIV measurements throughout the burning time of the SRM. However, the yield is affected in certain regions of the flow because of a non-homogeneous distribution of these ejected seed particles. This loss of vectors occurs in both regions of high particulate concentrations and also in regions where the number of particles is too scant.

The axial mean velocity profiles of the particulate phase show a tendency for self-preservation. In the range investigated (x/D = 11.0 to 18.5), plots of U/U_{max} plotted against r/x collapse into a single curve despite a two-phase, compressible, combustive and non-isothermal flow.

ACKNOWLEDGEMENTS

This work was supported by the Center for Simulation of Advanced Rockets, University of Illinois, Urbana-Champaign

REFERENCES

Adrian, R.J. (1991). "Particle-imaging techniques for experimental fluid mechanics", Annual Review of Fluid Mechanics, 23, 261-304.

Christodoulou, M., Eustace, R., Smith, T., Dennis, C.W. (2002), Personal Communication.

Deimling L. (1999). "Farbcodierte particle-image-velocimetry (PIV) zur diagnose von schnellen flammen", Ph.D. Thesis, Fraunhofer Institut Chemische Technologie.

Edwards, T., Horton, K.G., Redman, D., Rosa, J.S., Rubin, J.B., Yoon, S.C., Powers, J.P, Netzer, D.W. (1986), "Measurements of particulates in solid propellant rocket motors", 23rd JANNAF Combustion Meeting, Vol. 1., 1986.

Meinhart, C.D. (1994). "Investigation of turbulent boundary-layer structure using particle image velocimetry", Ph.D. Thesis, University of Illinois, Urbana-Champaign.

Stella, A., Guj, G., Kompenhans, J., Raffel, M., Richard, H. (2001). "Application of particle image velocimetry to combusting flows: design considerations and uncertainty assessment", Experiments in Fluids, 30, 167-180.

Yan, D., Zhang, J., He, A., Zhang, L. (1993). "Experimental studies on laser scattering from exhaust jet of a real rocket", Proc. SPIE Vol. 2005, "Optical diagnostics in fluid and thermal flow", Ed. Soyong S. Cha and James D. Trolinger, 1993, pp. 86-93.

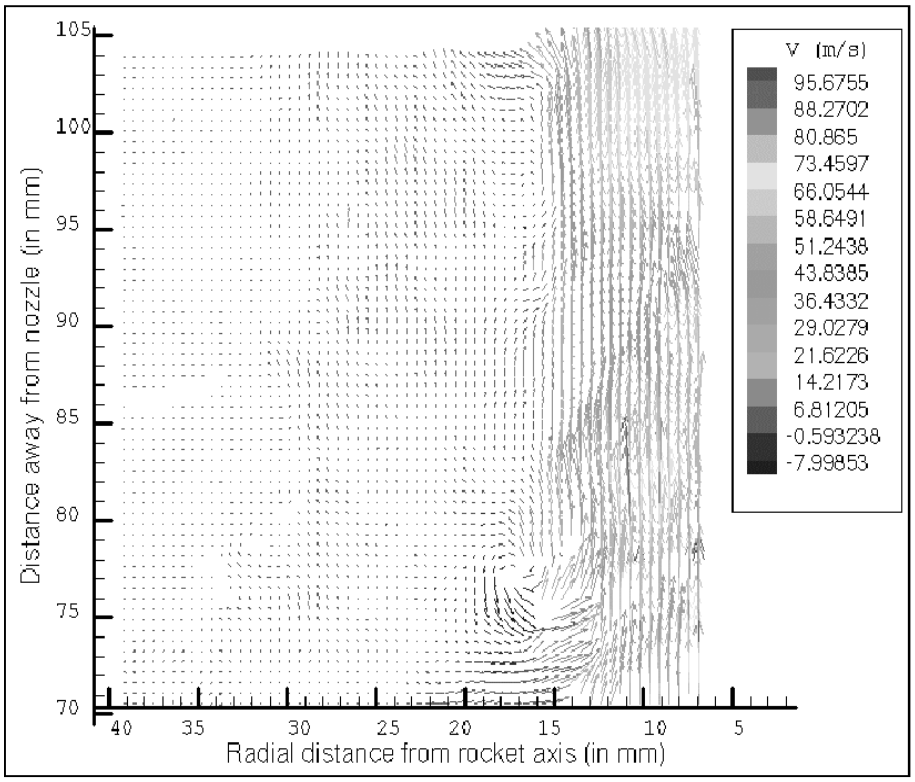

Fig 6. A PIV Image taken at t=0.033s showing the entrainment created by the emerging jet.

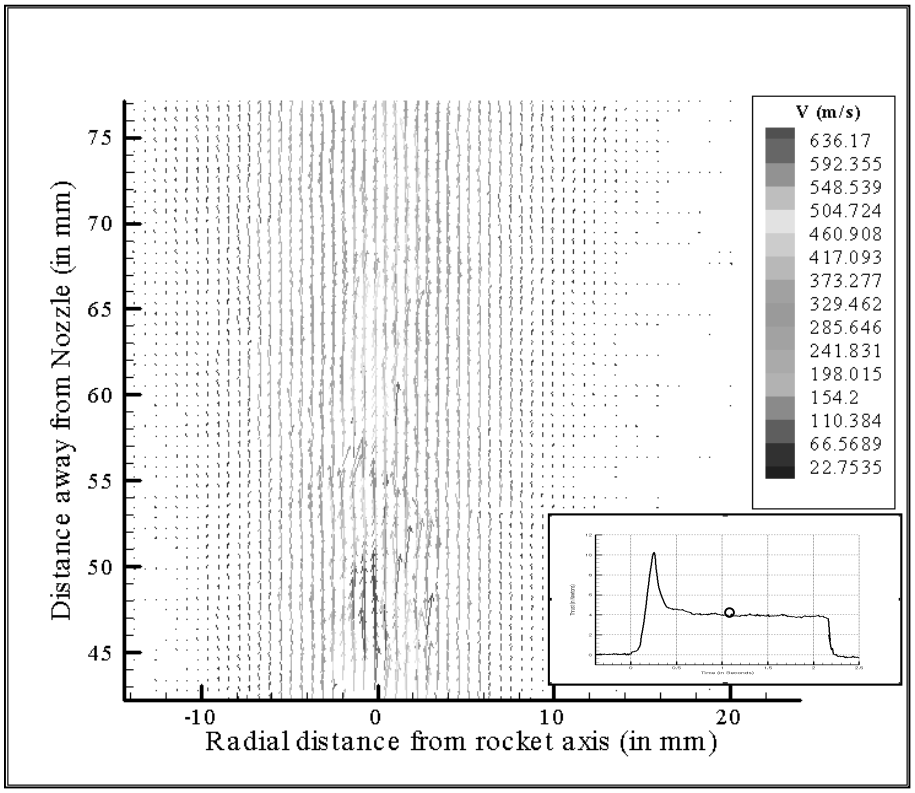

Fig 7. Ensemble Averaged velocity vector field at t=1.2s along with the thrust-time curve with the data point marked

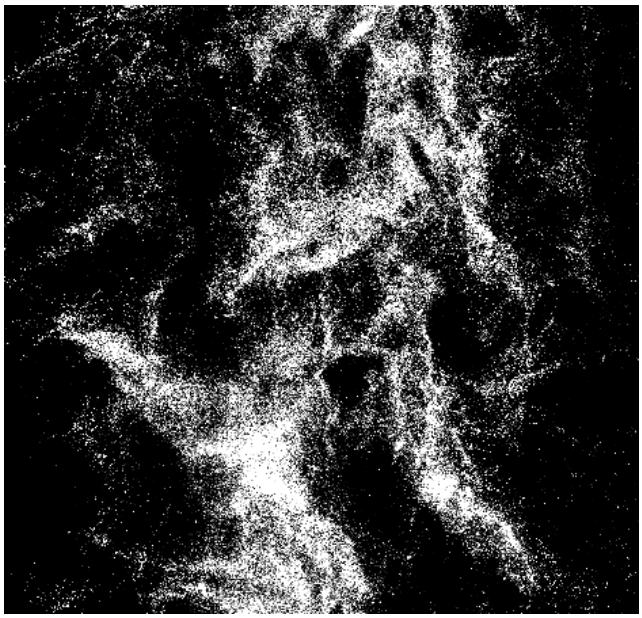

Fig 8. Segregation of the particulate into regions of high and low concentrations leads to a loss of vectors

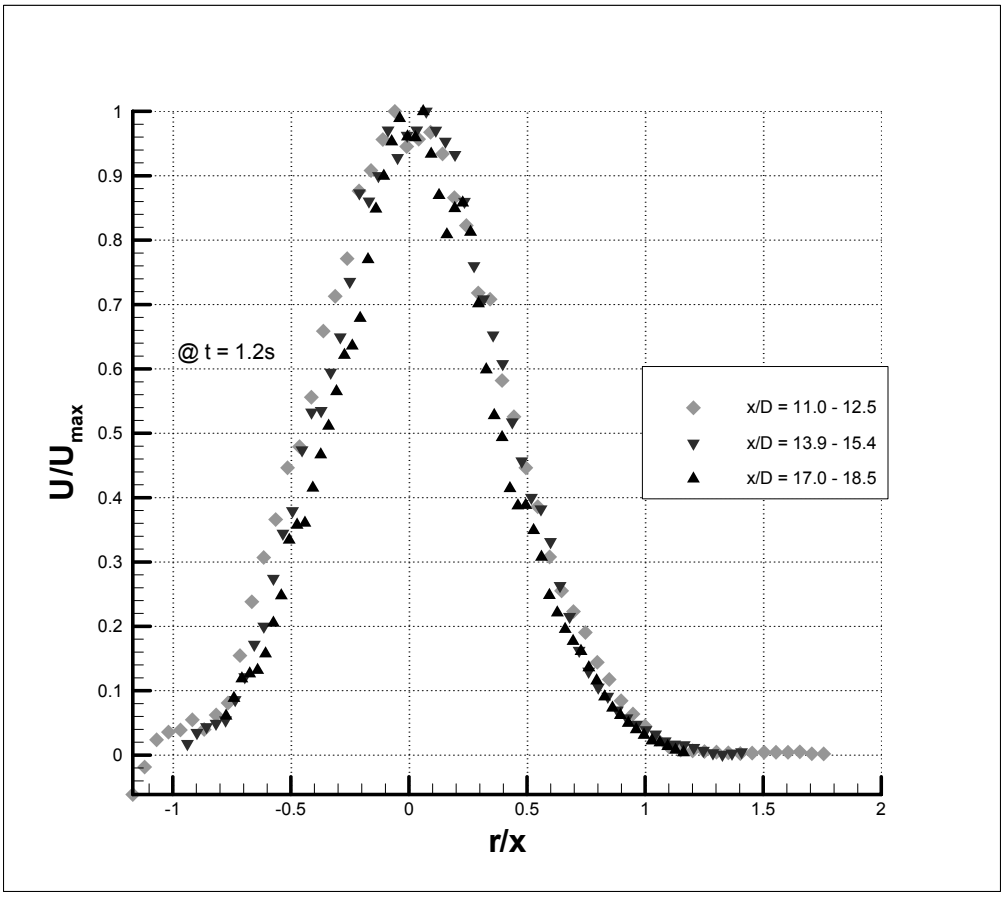

Fig 9. Self Similarity: Profiles of U/U_{max} plotted against r/x collapse into a single curve showing self similarity of the particulate-phase in the rocket flow. U_{max}=422m/s-608m/s